

Sizing of Hybrid Islanded Microgrids Using a Heuristic Approximation of the Gradient Descent Method for Discrete Functions

JC Oviedo*[‡], Johan S. Suarez**, C. Duarte***, J. Solano***

*Universidad Industrial de Santander, Ph.D. student

** Universidad Industrial de Santander, Assistant of research

*** Universidad Industrial de Santander, Associated professor

(juan.oviedo@correo.uis.edu.co, johan.suarez@correo.uis.edu.co, cedagua@uis.edu.co, jesolano@uis.edu.co)

[‡] Corresponding Author; First Author, Calle 9-27 Ciudad Universitaria, Bucaramanga, Colombia,

Tel: +57 316 246 6426, juan.oviedo@correo.uis.edu.co

Received: 20.11.2019 Accepted:06.01.2020

Abstract- Hybrid microgrids can handle fuel scarcity, reduce harmful emissions, increase flexibility, efficiency, and reliability. Nevertheless, these benefits are strongly related to the sizing and the energy management strategy (EMS) of the microgrid. In this regard, the sizing and the EMS acquire high importance for the planning of stand-alone microgrids. The present paper aims to design a sizing methodology that has a nested simulation model for power and energy balances. The sizing uses a heuristic approximation of the gradient descent method for discrete functions. The simulation model can evaluate the operation of the microgrid, even with EMSs using optimal criteria. A study case evaluation shows the effectiveness of the proposed algorithm compared to a traditional heuristic technique as Particle Swarm Optimization and an exhaustive search, which prove the feasibility of the algorithm to be used in stand-alone microgrid planning.

Keywords Hybrid microgrids, sizing, energy management, simulation, optimization.

1. Introduction

The benefits that the hybridization of different energy resources bring to stand-alone microgrids turn hybrid microgrids into an adequate solution for isolated geographical regions [1], [2]. Among these benefits, it is possible to mention that hybrid microgrids can manage better fuel scarcity, reduce harmful emissions, increase flexibility, efficiency, and reliability compared to microgrids run by mono generation facilities [3], [4]. Nonetheless, to obtain these benefits, the planning of the microgrid must consider the partially unpredictable nature and dependence on weather and climatic changes of the renewable energy resources[5], [6]. In this regard, the planning of stand-alone hybrid microgrids in rural areas requires the definition of the best sources of renewable energy according to the location, and the sizing of the generators and storage systems [7]–[10].

References [11], [12] define the sizing of stand-alone hybrid microgrids as the process of determining the size of each of the generators and storage systems to feed the demand

with a predefined desired reliability. The sizing generally wants to minimize investment costs, output energy costs, fuel consumption, or harmful environmental emissions among others [13], [14]. It is the sizing the responsible of unmet loads or excess of energy, which can affect directly the satisfaction of the customers or the investors. An under-sizing affects the comfort of the customers not providing enough energy when the customers expect to receive it. Unmet loads lead to unsatisfied customers, which can reduce their willingness to pay the fees [15], [16]. A reduction in the cash flow can start to deteriorate the project [17]. On the other hand, an over-sizing can cause a waste of energy, an extra investment cost and lack of economic return for the investors of the project due to the non-sold energy [18]. At the end, not only the reliability of the energy supply relies on proper sizing, but also the final cost of the energy. In this context, the sizing combination of stand-alone microgrids plays a vital role to achieve the success of the project [19], [20].

The sizing of the stand-alone microgrids is a complicated task since the accuracy of the results relies on the knowledge

$C_{x,k}^{min}$	Minimum value of capacity x	kW, kWh
$C_{x,k}^{med}$	Medium value of capacity x	kW, kWh
$C_{x,k}^{max}$	Maximum value of capacity x	kW, kWh
$\Delta C_{x,k}$	Capacity step for the search algorithm	kW, kWh
$TC_{x,k}$	Total operational costs	USD
$TFC_{d,h}$	Total fixed costs	USD
$TVC_{d,h}$	Total variable costs	USD
FC_{PV}	Fixed costs for the PV system	USD
FC_{DG}	Fixed costs for the Diesel generator	USD
FC_B	Fixed costs for the Battery Energy Storage System	USD
FC_{DLC}	Fixed costs of the Demand Management System	USD
r	Discount rate	Unitless
T	Period of simulation	Days
$TC_{x,k}^{P*}$	Partial minimum found at k iteration	kWh
$TC_{x,k}^S$	Total costs in the surroundings of the found minimum $TC_{x,k}^{P*}$	USD
$TC_{x,k}^*$	Final minimum found	USD
k	Iteration of the simulation	Unitless
γ_x	Weighting factor for the speed of convergence	Unitless
d	Day of the simulation	Days
h	Hour of the simulation	Hours
g	Defined gap to stop the search algorithm	Unitless
C_{DG}	Installed diesel capacity	kW
C_B	Installed storage capacity	kWh
C_{PV}	Installed photovoltaic system capacity	kW
C_{DLC}	Installed DLC system capacity	kW
II_{PV}	Unitary initial investment of the PV	USD/kW
II_{DG}	Unitary initial investment of the DG	USD/kW
II_B	Unitary initial investment of the storage	USD/kWh
II_{DLC}	Unitary initial investment of the DLC system	USD/kW
M_{PV}	Unitary maintenance costs of the PV	USD/kW-year
M_{DG}	Unitary maintenance costs of the DG	USD/kW-year
M_B	Unitary maintenance cost of the storage	USD/kW-year
M_{DLC}	Unitary maintenance cost of the DLC system	USD/kW-year
$TVCDG_{d,h}$	Total variable costs of the diesel generator	USD
π_L	Fuel price per liter	USD
$QDG_{d,h}$	Quantity of energy delivered by the diesel generator	kWh
$SOC_{d,h}$	State of charge of the Battery Energy Storage System	kWh
η_{in}	Efficiency of charge of the Battery	Unitless
η_{out}	Efficiency of discharge of the Battery	Unitless
$QBin_{d,h}$	Quantity of energy entering to the battery	kWh
$QBout_{d,h}$	Quantity of energy going out from the battery	kWh
$max(D_T)$	Maximum peak demand over the simulation horizon T	kW
$QDLC_{d,h}$	Quantity of energy curtailed by the DLC system	kWh
$CLE_{d,h}$	Cost of lack of energy	USD/kWh
$CEE_{d,h}$	Cost of excess of energy	USD/kWh
$QLE_{d,h}$	Quantity of energy not delivered to the demand	kWh
$QEE_{d,h}$	Quantity of excess energy produced by the system	kWh
β	Factor for the reliability of the microgrid	Unitless
$D_{d,h}$	Electrical demand at day d and hour h	kW
$QLOAD_{d,h}$	Quantity of energy requested by the load	kWh
$QPV_{d,h}$	Quantity of energy delivered by the PV system	kWh

Table 1 Variable declaration

of the technical specifications of the facilities, weather and climate conditions, and the characteristics of the load profiles [13], [21]. When there is no availability of weather and load forecasts, Neural Networks [22]–[25], Genetic Algorithms [26], [27] or hybrid neuro evolutionary methods can be useful to predict it [28]. In the cases where weather data is available; it is feasible to apply conventional techniques like the ones based on energy balances [29], or the ones that guarantee a predefined reliability level for the supply [30], [31].

Hafez et al. propose to use the software HOMER for the planning and optimal sizing of a hybrid renewable energy-based microgrid. The formulation aims to minimize the life-cycle cost while taking into account environmental emissions [7]. The main advantage of HOMER is its capacity of simulating different sizes of facilities and compare them considering the Levelized Cost of the Energy [32]. Homer executes a mixed simulation optimization approach using a hierarchical process. The lower level simulates and compute the operational costs. An intermediate level proposes the size of the energy sources to the lower level and finds the capacities with lower costs. Finally, the higher level performs sensitivity analysis for the main variables. Figure 1 represents the above.

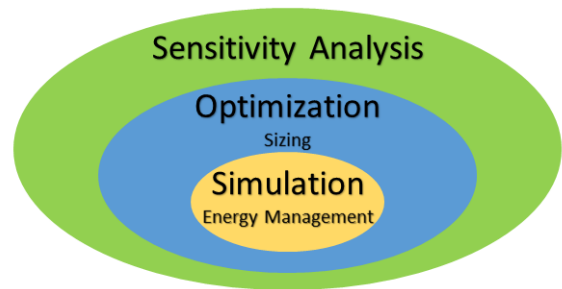


Figure 1 nested cycles of a mixed simulation optimization sizing methodologies.

The use of different Energy Management Strategies (EMS) based on rules allows HOMER to perform the dispatch of the energy resources in the microgrid. However, HOMER does not allow to apply any optimally designed EMS for the energy dispatch of the microgrid, which represents a considerable drawback [33]. Instead of using a search space as HOMER does, Sharafi et al. use a Particle Swarm Optimization formulation to find the size of the energy sources [34]. Despite that the proposed work allow the use of an optimal criterion for the sizing of the microgrid, any optimal criteria are applied for the EMS design.

In this regard, the main contribution of this paper is the formulation of a heuristic sizing methodology that mimic the behaviour of the gradient descent method for discrete functions and allows to apply any optimally designed dispatch strategy. In here is proposed a rule-based EMS that consider Direct Load Control (DLC) as a resource to curtail the demand of the microgrid only for its simplicity, but, any other optimal dispatch strategy will work as well. Results of the study case show a better speed of convergence and better accuracy for the proposed heuristic algorithm compared to Particle Swarm Optimization.

The description of the rest of the paper proceeds as follows: Section 2 presents the formulation of the considered problem. Section 3 presents the formulation of the sizing methodology. Section 4 presents the formulation of the economic dispatch strategy. Section 5 presents the simulations of a study case where the sizing methodology was applied. Finally, section 6 presents the conclusions of the work.

2. Problem modelling

The considered problem is the sizing of an islanded microgrid. The proposed solution is the design of a heuristic sizing methodology that mimics the behaviour of the gradient descent method. Even though the gradient descent method is an analytic technique designed to work with continuous and derivable functions, in here it is proposed an approach that simulates the behaviour of the gradient descent for discrete functions using three different steps. The first step is to create a search space defining limits for the capacities of the generators and storage systems of the facilities of the microgrid. A matrix *CM* is designed to store the installation and operational costs of the microgrid for the possible combinations of capacities of the facilities. Installation costs are obtained using the retail prices of the technologies in the market, and the operational costs are obtained simulating the operation of the microgrid over a predefined period *T*.

The second step is to execute a search methodology that proposes an initial point of evaluation inside of the search space and seeks in the surroundings for the maximum descent direction. After finding this direction, the algorithm actualizes the evaluation point; recompute the costs of the surroundings and re-evaluates the maximum descent direction. This process repeats until the algorithm finds a point where all the surroundings are higher than the evaluated point. The third step is to redefine the limits of the search space and tighten them around the found minimum point. Section 3 presents a further explanation of the sizing methodology.

A rule-based Energy Management Strategy is introduced to perform the simulations of the operation of the microgrid. Simulations are carried out assuming that it is possible to know one hour in advance the load and weather forecasts. The simulations are used to evaluate the reliability of the microgrid and estimate the operational costs, considering the combinations of the capacities used for the sizing algorithm. Section 4 further explain the rule-based EMS and the models of the generators and storage systems used for the simulations.

3. Sizing methodology

The proposed sizing methodology consists of three different steps. The creation of the search space is described in section 3.1. The search process is described in section 3.2. Finally, limits redefinition of the search space, are described in section 3.3.

3.1. Creation of the search space

To create the search space, it is proposed to build a matrix *CM* to store the total costs of the simulation results of using different combinations of capacities for the generators and

storage systems. This search space allows the reduction of a *x* dimension problem into a two-dimension problem, facilitating a graphical inspection of the minimum of the objective function. To build the matrix *CM* any number of *n* steps between $C_{x,k}^{min}$ and $C_{x,k}^{max}$ can be used. Increasing the number of steps will increase the computational time, but also will increase the accuracy of the algorithm. Finding the number of *n* steps that will represent a good compromise between simplicity, speed of convergence and accuracy is leave out of the scope of this work. In here, for explanation purposes, it is proposed to use three different evaluation points for each capacity: $C_{x,k}^{min}$, $C_{x,k}^{med}$ and $C_{x,k}^{max}$ to build the matrix *CM*. The three different points are equally separated by a predefined step $\Delta C_{x,k}$. The relations between the three points and the step are described in Equations (1) to (4).

$$C_{x,k}^{min} \geq 0 \tag{1}$$

$$\Delta C_{x,k} \geq 0 \tag{2}$$

$$C_{x,k}^{med} = C_{x,k}^{min} + \Delta C_{x,k} \tag{3}$$

$$C_{x,k}^{max} = C_{x,k}^{med} + \Delta C_{x,k} \tag{4}$$

$$x = (PV, B, DG, DR) \tag{5}$$

Using the proposed method is possible to reduce a *x* dimension space into a two-dimension space to build the matrix *CM*. Figure 2 illustrates the results of the dimension reduction of a four-dimension space into two-dimension space.

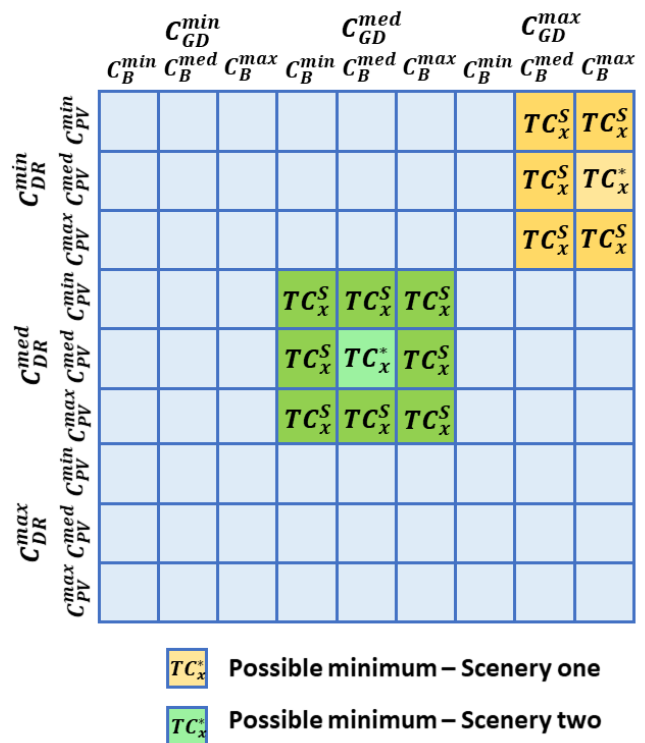


Figure 2 Matrix *CM*, designed to store the total costs of installation and operation of the islanded microgrid.

The values inside of matrix *CM* are the sum of the fixed and variable costs, and they are computed using Equation (6).

$$TC_{x,k} = \sum_{d=1}^T \sum_{h=1}^{24} TFC_{d,h} + TVC_{d,h} \quad (6)$$

The total fixed costs $TFC_{d,h}$ are related to the installation costs of the technologies as described by equation (7) and further explained in section 4.1.

$$TFC_{d,h} = (FC_{PV} + FC_{DG} + FC_B + FC_{DLC})(1+r)^{\frac{T}{365}} \quad (7)$$

The total variable costs $TVC_{d,h}$ are obtained from the simulations of the operation of the microgrid, using the combination of capacities $C_{x,k}^{min}$, $C_{x,k}^{med}$ and $C_{x,k}^{max}$ as described in Section 4.

3.2. Search algorithm

To find the minimum installation and operational costs inside of the search space, it will be enough to compute all the possible combinations of the matrix CM . Doing so, it will be possible to guarantee the global minimum inside of the search space. However, this will lead to the curse of dimensionality, increasing the computational time of the problem. Instead of doing so, it is proposed to generate a search particle that will start from a random configuration of the capacities $C_{x,k}^{min}$, $C_{x,k}^{med}$ and $C_{x,k}^{max}$ and compute the costs of this initial point $TC_{x,k}^0$. Afterward, the algorithm computes the costs of the surrounding combinations $TC_{x,k}^S$. Once $TC_{x,k}^0$ and $TC_{x,k}^S$ are known, a comparison of the values is used to find the maximum descent direction. This process repeats until the algorithm finds a minimum point $TC_{x,k}^*$, where the costs of all the surroundings $TC_{x,k}^S$ are higher. Figure 3 shows a representation of the proposed search process.

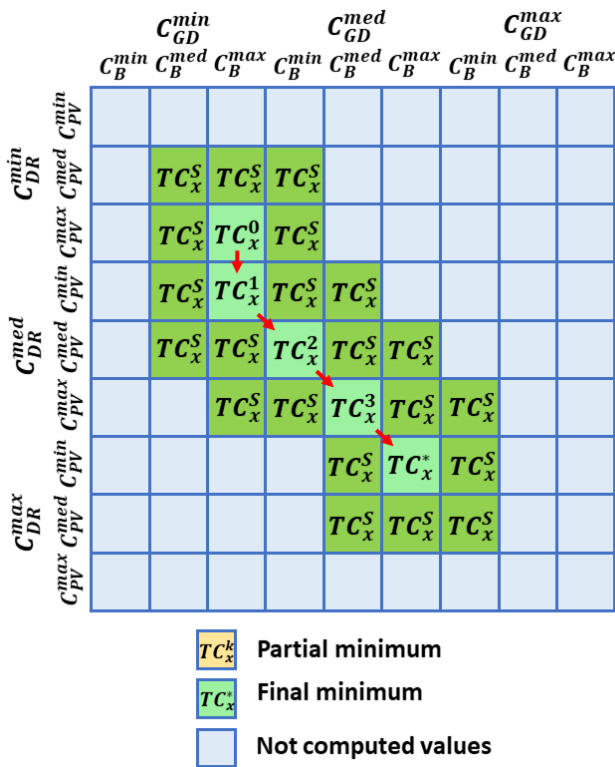


Figure 3 Graphical description of the search process.

To avoid the search algorithm being trap in a local minimum two actions can be done. The first is to perform a visual inspection of the objective function by creating a 3D plot, as shown in Figure 4. The second is to increase the number of search particles to a defined N number. Afterwards, compare the results of all the N particles choosing the best achieved minimum to redefine the limits of the search space around it. Finding the number of N particles that will represent a good compromise between simplicity, speed of convergence and accuracy is leave out of the scope of this work.

3.3. Redefining the search space

The limits of the matrix CM are modified once the minimum costs $TC_{x,k}^*$ are found. The modification of the lower limit $C_{x,k}^{min}$ and the higher limit $C_{x,k}^{max}$ is designed to tighten the search space around the minimum point $TC_{x,k}^*$. As illustrated in Figure 2, two possible scenarios are considered for the actualization of the limits: if the found minimum is in the borders or if it is inside of the matrix CM .

3.3.1. Minimum cost in the borders of the matrix CM

If the localization of the minimum is at the borders of the matrix CM , the search space moves in the same direction of the found limit without modifying the step. Equation (8) and (9) describe the process:

$$C_{x,k}^{min} = C_{x,k-1}^{min} \pm \Delta C_{x,k} \quad (8)$$

$$\Delta C_{x,k} = \Delta C_{x,k-1} \quad (9)$$

The sign \pm will be positive if the minimum is in a superior border $C_{x,k}^{max}$ or negative if the minimum is in an inferior border $C_{x,k}^{min}$.

3.3.2. Minimum cost inside of the matrix CM

If the localization of the minimum is inside of the matrix CM , the search space tightens around the minimum point. Equations (10) to (13) describes the actualization process.

$$C_{x,k}^{min} = C_{x,k-1}^{min} + \gamma_x \Delta C_{x,k} \quad (10)$$

$$\Delta C_{x,k} = (1 - \gamma_x) \Delta C_{x,k-1} \quad (11)$$

$$\gamma_x = \gamma_{PV}, \gamma_B, \gamma_{GD}, \gamma_{DLC} \quad (12)$$

$$0 < \gamma_x < 1 \quad (13)$$

The x coordinates of the new medium point $C_{x,k}^{med}$ are the same coordinates as the $C_{x,k-1}^{med}$. The γ_x factor is introduced to control the speed of convergence of the proposed search algorithm. γ values closer to one will increase the speed of convergence but will reduce the accuracy to find the minimum point. γ values closer to zero will reduce the speed of convergence, increasing the number of k required iterations to find the minimum point $TC_{x,k}^*$ but it will increase the accuracy to find the minimum point.

3.3.3. Stops criteria

The algorithm stops to redefine the limits of search space when the difference between the minimum cost $TC_{x,k}^*$ and the cost in the surroundings $TC_{x,k}^S$ is less than a predefined gap.

$$TC_{x,k}^* - TC_{x,k}^S < g \quad (14)$$

3.4. Possible combinations of all the capacities

The combination of the capacities introduced by Equation (5) and illustrated in Figure 2 is not the only possible one. A cartesian product is used to find all the possible combinations that matrix CM can have and eliminate the equivalent combinations. A mathematical notation is proposed for CM to facilitate the understanding of the results:

Parameter	Mathematical form
Exterior capacity file	F
Interior capacity file	f
Exterior capacity column	C
Interior capacity column	c

Table 2 Proposed mathematical notation

The cartesian product is performed using the two following groups:

$$Pos = (F, f, C, c) \quad (15)$$

$$x = (PV, B, DG, DR) \quad (16)$$

Table \ref{table:2} presents the results of the cartesian product between Pos and x after eliminating the equivalent combinations.

- | | |
|---------------------------------|---------------------------------|
| 1. $F_{PV} f_{dg} C_B c_{dlc}$ | 2. $F_{GD} f_{pv} C_B c_{dlc}$ |
| 3. $F_{PV} f_{dg} C_{DLC} c_b$ | 4. $F_{GD} f_{pv} C_{DLC} c_b$ |
| 5. $F_{DG} f_b C_{PV} c_{dlc}$ | 6. $F_B f_{dg} C_{PV} c_{dlc}$ |
| 7. $F_{DG} f_b C_{DLC} c_{pv}$ | 8. $F_B f_{dg} C_{DLC} c_{pv}$ |
| 9. $F_{PV} f_b C_{DLC} c_{dg}$ | 10. $F_B f_{pv} C_{DLC} c_{dg}$ |
| 11. $F_{PV} f_b C_{DG} c_{dlc}$ | 12. $F_B f_{pv} C_{DG} c_{dlc}$ |

Table 3 Possible combinations.

Due to the reduction of the x dimensions into two dimensions, it is possible to visualize the objective function. Combinations of Table 3 are plotted in Figure 4.

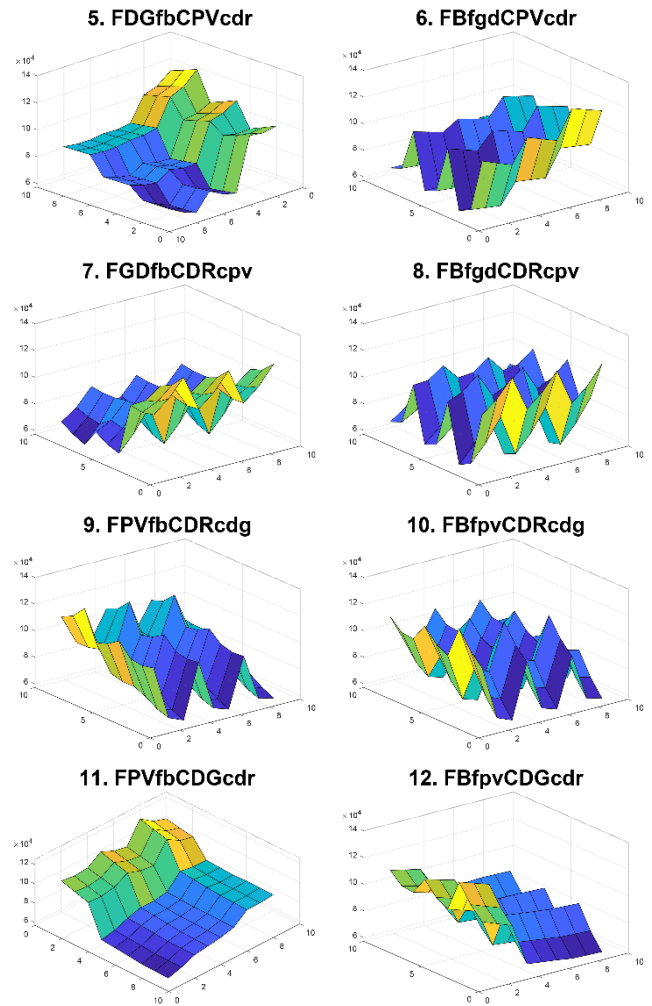
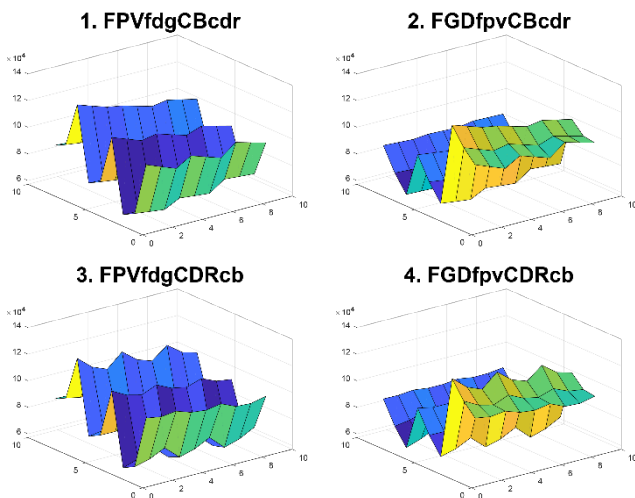


Figure 4 Possible combinations of the different capacities for the sizing.

4. Energy management strategy design

An Energy Management Strategy (EMS) is designed to evaluate if the installed capacities are enough to fulfil the demand during the time. The EMS includes a direct load control management strategy that allows the disconnection of a percentage of the load if it is needed. The EMS is designed using the economic dispatch theory to define the order and the quantities in which the generators should be dispatched using an hourly step. For each hour of operation, the algorithm computes the marginal costs of all the available generation resources and selects the less expensive to be dispatched.

It is worth it to notice that the EMS is designed to consider a DG. However, other sources, such as gas, biogas, biodiesel generator, or even fuel cells can be considered using the proposed sizing methodology. Section 4.1 presents the cost model of the DG which depends on the size and the diesel consumption. Cost models are similar in sources such as fuel cells where the cost depends on the size and hydrogen consumption. Section 4.1 additionally presents the models used to compute the costs of all the generation and storage technologies considered for the microgrid.

4.1. Models of the generators and storage system

4.1.1. Photovoltaic system

The photovoltaic system costs are related to the initial investment and the maintenance of the system:

$$FC_{PV} = C_{PV}I_{PV} + C_{PV}M_{PV} \quad (17)$$

The variable costs of the photovoltaic system are assumed to be zero after its installation [35], [36].

4.1.2. Diesel Generator

The diesel generator fixed costs are related to the initial investment and the maintenance of the system:

$$FC_{DG} = C_{DG}I_{DG} + C_{DG}M_{DG} \quad (18)$$

Equation (19) express diesel consumption as a function of the installed capacity and output power.

$$TVCDG_{d,h} = \pi_L C_{DG} \left(\frac{0.024QDG_{d,h}}{C_{DG}} + 0.031 \right) \quad (19)$$

Equation (20) describes the generation limits:

$$0.3C_{(GD)} \leq QDG_{(d,h)} \leq 0.9C_{(GD)} \quad (20)$$

4.1.3. Battery Energy Storage System

Battery fixed costs are related to its installation and maintenance:

$$FC_B = C_B I_B + C_B M_B \quad (21)$$

The variable costs of the BESS are assumed to be zero. Equation (22) describes the state of charge of the battery. Equations (23) and (24) describes the dynamics of charging and discharging the battery. Equation (25) describes the allowed variation of the state of charge of the battery.

$$SOC_{d,h} = SOC_{d,h-1} + \eta_{in} QBin_{d,h} - \frac{QBout_{d,h}}{\eta_{out}} \quad (22)$$

$$-0.3C_B \leq QBin_{d,h} \leq 0 \quad (23)$$

$$0 \leq QBout_{d,h} \leq 0.3C_B \quad (24)$$

$$0.4C_B \leq SOC_{d,h} \leq 0.9C_B \quad (25)$$

4.1.4. Direct Load Control System

The direct load control fixed costs are related to the initial investment to acquire the technology and its maintenance.

$$FC_{DLC} = C_{DLC}I_{DLC} + C_{DLC}M_{DLC} \quad (26)$$

Equation (27) define the limits of curtailed energy by the DLC strategy.

$$-0.1max(D_T) < QDLC_{d,h} < 0 \quad (27)$$

4.1.5. Excess and lack of energy modelling

A cost CEE is introduced to weight the energy that the generation facilities provide, but it is not possible to consume by the demand. A cost CLE it is proposed to weight the power that the customers require, but the generation facilities are not able to produce. Equations (28) an (29) define both costs:

$$CEE = \beta QEE_{(d,h)} \quad (28)$$

$$CLE = \beta QLE_{(d,h)} \quad (29)$$

$$\beta > 1 \quad (30)$$

Where β is a weighting factor that can be tuned to guarantee a certain degree of reliability for the microgrid.

4.2. Scenarios for the EMS

Three possible scenarios are considered to formulate the EMS, when the PV generation is zero ($PV_{d,h} = 0$), when is greater than zero and smaller than the load ($0 < PV_{d,h} < QLOAD_{d,h}$), and when is greater that the load ($PV_{d,h} > QLOAD_{d,h}$). The three scenarios are explained in Section 4.2.1, 4.2.2 and 4.2.3, respectively.

4.2.1. Photovoltaic generation equal to zero

Variable costs of each technology are obtained to estimate the order of the dispatch. The most economical technology between the DG and the BESS is dispatched first, considering the minimum and maximum power dispatch for the DG and the BESS. The second most economical technology is dispatched afterward considering the maximum and minimum power outputs. The DLC is used only in the case that the DG and the BESS are not enough to supply the demand.

4.2.2. Photovoltaic generation greater than zero and smaller than the demand

If the PV generation is greater than zero and smaller than the load, the total demand $D_{d,h}$ can be expressed as:

$$D_{\{d,h\}} = QLOAD_{\{d,h\}} - QPV_{\{d,h\}} \quad (31)$$

The DG, BESS, and DLC must serve the demand $D_{d,h}$. In case that the DG, BESS, and DLC working at its maximum capacities are not enough to feed it, the rest will be considered as a lack of energy. Variable QLE will store all the shortages.

4.2.3. Photovoltaic generation bigger than the demand

The BESS stores the excess of energy produced by the PV. A rule is designed to avoid overpassing the maximum charge rate capacity Qin_{max} of the battery. If the power generated for the PV is higher than Qin_{max} , the BESS will take only its maximum capacity rate of charge, and the rest is considered a waste of energy. Variable QEE will record all the excesses of energy. Figure 5 illustrates the three possible scenarios for the dispatch.

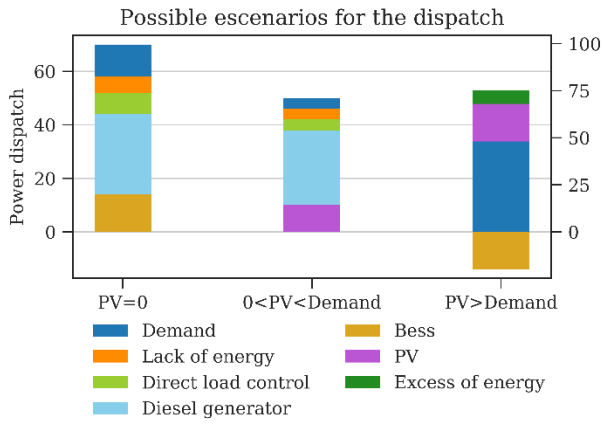


Figure 5 Order to dispatch the energy sources.

5. Simulations and results

In this section, numerical examples are provided to illustrate the performance of the proposed method. The study case is the sizing of a hypothetical microgrid located at longitude 77° 16' 8" West and latitude 5° 41' 36" North (Nuquí, Colombia). The microgrid will be composed of Photovoltaic panels (PV), a Battery Energy Storage System (BESS), a Diesel Generator (DG) and a Direct Load Control (DLC) system. The maximum load of the considered microgrid is 460 kW. Instituto de Hidrología, Meteorología y Estudios Ambientales (IDEAM), a Colombian institute in charge of monitoring the weather across the country, provides meteorological data for the simulations. The average Global Horizontal Irradiance (GHI) in Nuquí is 3,5 kWh/m². The cost of Diesel used for the simulations is 0.79 USD/liter. Table \ref{tabla:6} summarizes the unitary costs used for the simulations.

System	Initial investment	Maintenance	Operation
PV	1300 USD/kW	0.02 USD/kW	0 USD
BESS	420 USD/kWh	0.01 USD/kWh	0 USD
DG	550 USD/kWh	0.75 USD/kWh	Equation (16)
DLC	50 USD/kW	0 USD/kW	0 USD

Table 4 Unitary system costs for simulations.

The obtained results of the proposed algorithm are compared to the results of a Particle Swarm Optimization (PSO) and an Exhaustive Search Algorithm. The application of the PSO algorithm is explained in section 5.1. The implementation of the exhaustive search algorithm is described in section 5.2. Section 5.3 presents the results of the proposed algorithm. Finally, a comparison between the three algorithms is explained in section 5.4.

5.1. Particle swarm optimization algorithm

PSO is a stochastic optimization algorithm that is based in the animal migration process [37], and is described in equations (32) and (33).

$$\mathbf{v}_i^{k+1} = w\mathbf{v}_i^k + c_1 \text{rand}_1 \mathbf{Pbest}_i - \mathbf{x}_i^k + c_2 \text{rand}_2 \mathbf{Gbest} - \mathbf{x}_i^k \quad (32)$$

$$\mathbf{x}_i^{k+1} = \mathbf{x}_i^k + \mathbf{v}_i^{k+1} \quad (33)$$

Where \mathbf{x}_i^k represents the i^{th} particle at k iteration. \mathbf{Pbest}_i is the personal best position of the i^{th} particle and \mathbf{Gbest} is the global best position of the group of particles. c_1 and c_2 are positive constants, and rand_1 and rand_2 are random numbers with uniform distribution between $[0,1]$. \mathbf{v}_i^k is the velocity vector of the i^{th} particle and w is the inertial factor. The implementation of PSO algorithm for the sizing of islanded microgrids is shown in figure \ref{fig:algo}.

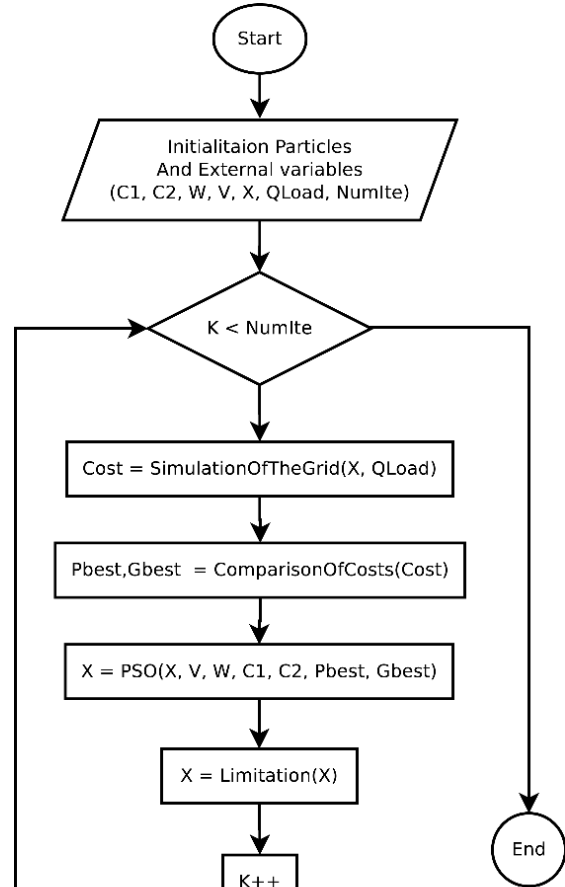


Figure 6 Diagram of the PSO algorithm implementation.

5.1.1. Initialization of the algorithm

The PSO algorithm starts setting the values of the constants w , c_1 and c_2 ; the particle position matrix \mathbf{x}^k and velocity vector \mathbf{v}^k ; the load of the islanded microgrid $QLoad$, and the number of iterations $NumIte$. Equation (34) presents \mathbf{x}^k , where the rows are the variables to optimize and the columns are the particles.

$$\mathbf{x}^k = \begin{bmatrix} CPV_1^k & CPV_1^k & \dots & CPV_i^k \\ CBESS_1^k & CBESS_2^k & \dots & CBESS_i^k \\ CGD_1^k & CGD_2^k & \dots & CGD_i^k \\ CDLC_1^k & CDLC_2^k & \dots & CDLC_i^k \end{bmatrix} \quad (34)$$

The accuracy of the PSO depends on the tuning of the constants, c_1 , c_2 and w . To avoid the tuning of this parameters, we use the recommended values of the work presented in [38], where c_1 and c_2 are equal to "2", and w between $[0.4,0.9]$.

5.1.2. Internal computations of the algorithm

Using the rule-based EMS presented in Section 4 is created the function *SimulationOfTheGrid()*. The inputs of this function are the capacities of the energy sources that the sizing algorithm defines. Afterwards, a comparison cost is performed with the function *ComparisonOfCost()*. This function finds the *Gbest* and *Pbest*. A third function *PSO()* is introduced to compute equations (32) and (33). Finally, the function *Limitation()* keep the variation of the particles inside of the search space.

5.1.3. Stops criteria

An external function is defined to maintain the algorithm iterating until it reaches the predefined number of iterations. Despite that more sophisticated stopping criterions could be computed; the simplicity of this strategy makes it a proper candidate. However, the number of iterations was selected after the algorithm reach's global minimum found with the exhaustive search. Figure 7 presents the sizing results using the PSO algorithm.

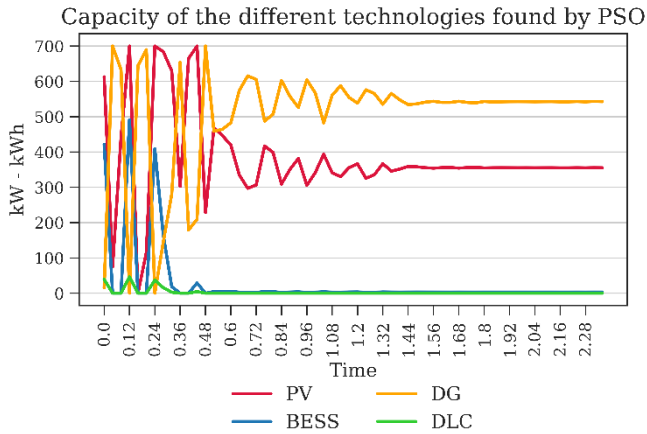


Figure 7 PSO sizing results.

5.2. Exhaustive search

An exhaustive search was performed to verify if the proposed algorithm and the PSO algorithm are converging to the global minimum of the evaluation function. The exhaustive search makes a thin discretization of the search space for each of the generators and storage systems for the microgrid [39], [40]. Afterwards, a cartesian product is applied to find all the possible combinations of the C_{PV} , C_{BESS} , C_{DG} , and C_{DLC} . *SimulationOfTheGrid()* computes the operational costs of the microgrid for each possible combination. Figure 8 presents the results obtained using the exhaustive search algorithm.

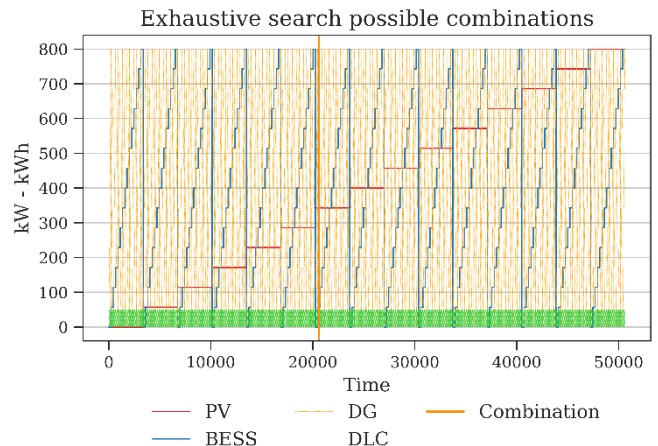


Figure 8 Exhaustive search sizing results.

5.3. Proposed algorithm

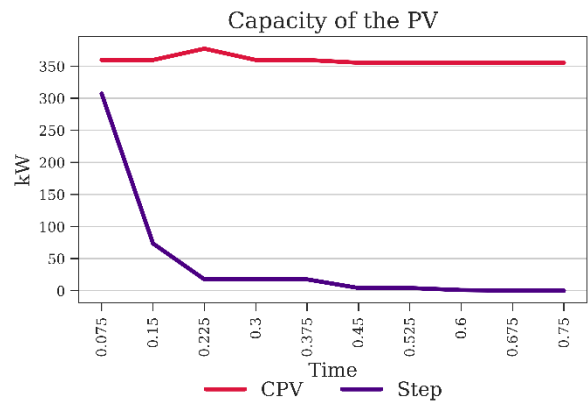
As described in section 3, different organizations of the capacities can be chosen to build the matrix CM . Due to the heuristic characteristic of the proposed algorithm, it is desirable to adopt a combination that avoids the search process be trap in a local minimum. In this regard, the combination 11 was selected to perform the simulations.

The first step of the proposed algorithm is to define the search space, and the second is to execute the search process. However, these two processes depend on $C_{x,k}^{min}$, $\Delta C_{x,k}$, $C_{x,k}^{max}$ and γ_x . To avoid subjectivities in the selection of these parameters, they were not chosen randomly. Instead, a Genetic Algorithm (GA) was used to find the initial points, steps, and the γ_x factor. Table 5 show the results.

System	$C_{x,k}^{min}$	$\Delta C_{x,k}$	$C_{x,k}^{max}$	γ_x
PV	52 kW	300 kW	652 kW	0.2397
BESS	244 kWh	178 kWh	600 kW	0.2629
DG	304 kW	131 kW	566 kW	0.2585
DLC	34 kW	8 kW	50 kW	0.6743

Table 5 Initial values of the parameters for the proposed algorithm.

Using the above-mentioned parameters, the proposed algorithm converges after ten iterations. Figure 9 illustrates how the minimum capacity is modified and how the step reduces its size each k iteration.



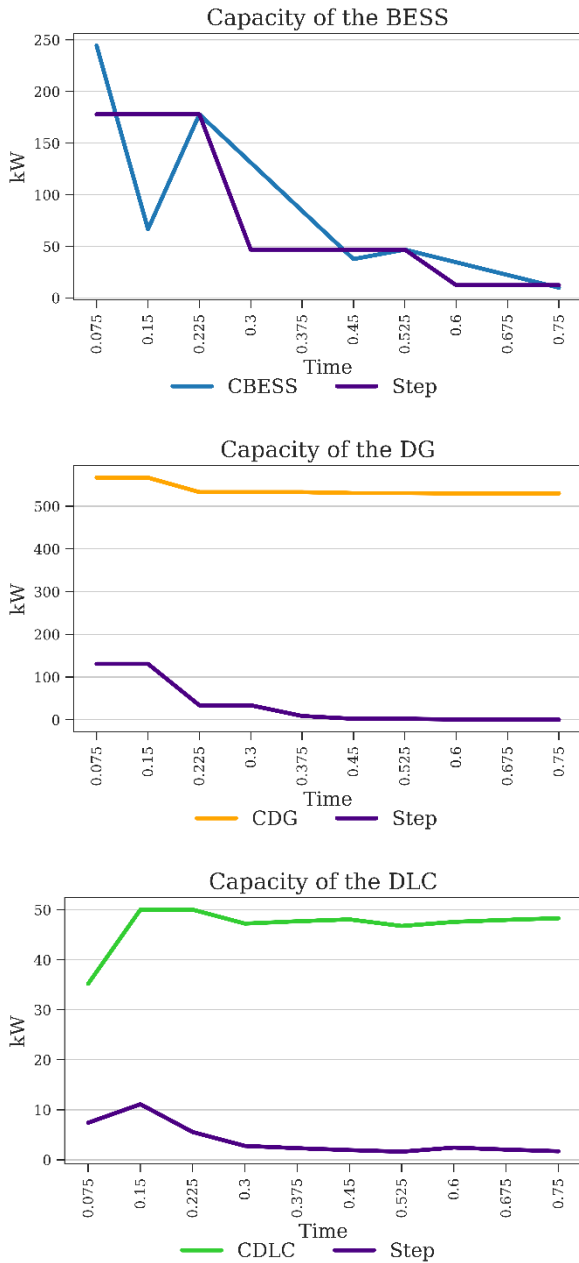


Figure 9 Proposed algorithm sizing results.

5.4. Comparison between the three algorithms

To make the comparisons of the algorithms, three different aspects were analysed: speed of convergence, best-achieved minimum, and physical computational cost. Section 5.4.1 present the comparison of the speed of convergence of the proposed algorithm and the PSO. Section 5.4.2 shows the best minimum achieved for each of the algorithms. Finally, Section Error! Reference source not found. presents the physical computational cost required to execute the algorithms. The configuration of the software used for the simulations and the characteristics of the computer are described in Table 6.

Parameter	Data
Date/hour	28-Jun-2019/09:52:25
MATLAB version	9.5.0.944444 (R2018b)
MATLAB accelerator	Enabled
MATLAB JIT	Enabled

MATLAB assertions	Disabled
MATLAB Desktop	Enabled
Java JVM	Enabled
Java version	Java 1.8.0_152-b16
CPU	x86 Intel Core i5 8250u
Operative system	Microsoft Windows 10
Number of cores	4
Number of threads	4

Table 6 Matlab and test computer configuration information.

5.4.1. Speed of convergence

Figure 10 shows how the values of the capacities found with the PSO and the proposed algorithm evolves in time, and how much far are they from the global minimum found with the exhaustive search.

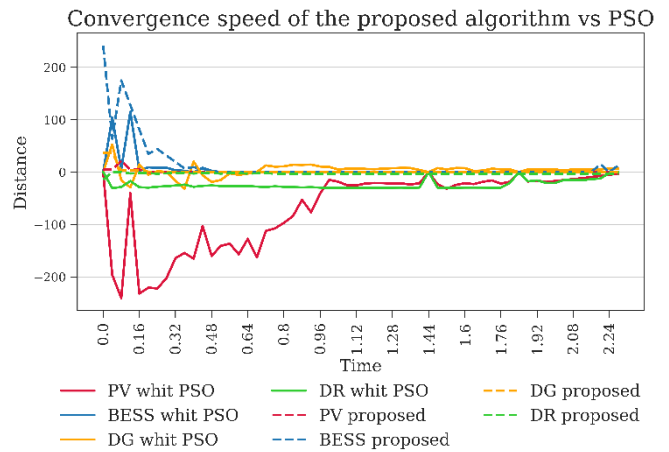


Figure 10 Convergence of the algorithms.

5.4.2. Best achieved minimum

The best-achieved minimum for each of the used algorithms in the comparisons is presented in Table 7.

Parameter	Exhaustive search	PSO	Proposed	Units
PV	355	331	342	kW
BESS	3	3	3	kWh
DG	526	538	530	kW
DLC	50	43	46	kW
Time	16.483	1.5628	0.7518	Seconds
Total cost	49101	50932	50232	USD

Table 7 Comparison of results

The proposed algorithm converges around two times faster than the PSO and twenty times faster than the exhaustive search. However, the found solution is approximately 2.5% more expensive than the solution found with the exhaustive search.

6. Conclusion

This paper presents the formulation of a sizing methodology for islanded microgrids using a heuristic approximation of the gradient descent method for discrete functions. The methodology uses simulations of different combinations of capacities of generators and storage systems to evaluate the ability of the combinations to feed the electrical demand of the islanded microgrid. Three steps are used to converge to a minimum point: delimiting the feasible region, a search process, and redefining the limits of the search space.

The main benefit of the proposed methodology is the ability to add the possibility of using an EMS that optimally dispatches the resources of the microgrid to a simulation model. The method proves to be faster and to provide a better minimum value than Particle Swarm Optimization. However, further comparisons against other heuristic methodologies are required.

To avoid relying on the designers' previous knowledge, a Genetic Algorithm was used to delimit the feasible region of the search space for the study case. The study case results show the effectiveness of the proposed sizing methodology. Despite this, some considerations of the algorithm are worth to be noticed. The algorithm does not address the effects of the uncertainties introduced by the forecast of the solar radiation and the electrical demand. Additionally, the accuracy of the algorithm is highly dependent on the definition of the feasible region to start the search process, the γ_x factors introduced to regulate the speed of convergence, and the selection of the possible combinations to create the search space. In this regard, the genetic algorithm improves the final results, but if these factors are left to the criteria of the designer, the algorithm loses accuracy and speed of convergence. All these aspects must be evaluated and improved in further works.

Acknowledgements

Authors may acknowledge to any person, institution or department that supported to any part of study.

References

- [1] Z. Xu, M. Nthontho, and S. Chowdhury, "Rural electrification implementation strategies through microgrid approach in South African context," *Int. J. Electr. Power Energy Syst.*, vol. 82, pp. 452–465, 2016.
- [2] Y. Mekonnen and A. I. Sarwat, "Renewable energy supported microgrid in rural electrification of Sub-Saharan Africa," *Proc. - 2017 IEEE PES-IAS PowerAfrica Conf. Harnessing Energy, Inf. Commun. Technol. Afford. Electrification Africa, PowerAfrica 2017*, pp. 595–599, 2017.
- [3] P. Bajpai and V. Dash, "Hybrid renewable energy systems for power generation in stand-alone applications: A review," *Renew. Sustain. Energy Rev.*, vol. 16, no. 5, pp. 2926–2939, 2012.
- [4] C. E. Casillas and D. M. Kammen, "The delivery of low-cost, low-carbon rural energy services," *Energy Policy*, vol. 39, no. 8, pp. 4520–4528, 2011.
- [5] W. Zhou, C. Lou, Z. Li, L. Lu, and H. Yang, "Current status of research on optimum sizing of stand-alone hybrid solar – wind power generation systems," *Appl. Energy*, vol. 87, no. 2, pp. 380–389, 2010.
- [6] C. Li *et al.*, "Comprehensive review of renewable energy curtailment and avoidance: A specific example in China," *Renew. Sustain. Energy Rev.*, vol. 41, pp. 1067–1079, 2015.
- [7] O. Hafez and K. Bhattacharya, "Optimal planning and design of a renewable energy based supply system for microgrids," *Renew. Energy*, vol. 45, pp. 7–15, 2012.
- [8] N. Zhou, N. Liu, J. Zhang, and J. Lei, "Multi-objective optimal sizing for battery storage of PV-based microgrid with demand response," *Energies*, vol. 9, no. 8, pp. 1–24, 2016.
- [9] Y. LI and F. NEJABATKHAH, "Overview of control, integration and energy management of microgrids," *J. Mod. Power Syst. Clean Energy*, vol. 2, no. 3, pp. 212–222, 2014.
- [10] B. Li, R. Roche, D. Paire, and A. Miraoui, "Sizing of a stand-alone microgrid considering electric power, cooling/heating, hydrogen loads and hydrogen storage degradation," *Appl. Energy*, vol. 205, no. July, pp. 1244–1259, 2017.
- [11] G. Notton, V. Lazarov, Z. Zarkov, and L. Stoyanov, "Optimization of hybrid systems with renewable energy sources: Trends for research," in *1st International Symposium on Environment Identities and Mediterranean Area, ISEIM*, 2006, pp. 144–149.
- [12] J. L. Bernal-Agustín and R. Dufo-López, "Simulation and optimization of stand-alone hybrid renewable energy systems," *Renew. Sustain. Energy Rev.*, vol. 13, no. 8, pp. 2111–2118, 2009.
- [13] A. Maheri, "Multi-objective design optimisation of standalone hybrid wind-PV-diesel systems under uncertainties," *Renew. Energy*, vol. 66, pp. 650–661, 2014.
- [14] V. Amir, S. Jadid, and M. Ehsan, "Optimal Planning of a Multi-Carrier Microgrid (MCMG) Considering Demand-Side Management," *Int. J. Renew. Energy Res.*, vol. 8, no. 1, 2018.
- [15] REN 21, *Renewables 2019 Global Status Report*. 2019.
- [16] S. R.-Álvarez, J. Patiño, A. Márquez, and J. Espinosa, "Optimal Design for an Electrical Hybrid Micro Grid in Colombia Under Fuel Price Variation," *Int. J. Renew. Energy Res.*, vol. 7, no. December, 2017.
- [17] D. Schnitzer, Deepa Shinde Lounsbury, J. P. Carvallo, R. Deshmukh, J. Apt, and D. M. Kammen, "Microgrids for Rural Electrification: A critical review of best practices based on seven case studies," 2014.
- [18] N. J. Williams, P. Jaramillo, J. Taneja, and T. S. Ustun, "Enabling private sector investment in microgrid-based rural electrification in developing countries: A review," *Renew. Sustain. Energy Rev.*, vol. 52, pp. 1268–1281, 2015.
- [19] T. S. U. Andrew Harrison Hubble, "Hybrid Mini-Grids for Rural Electrification," 2016.
- [20] P. Ciller, F. De Cuadra, and S. Lumbreras, "Optimizing Off-Grid Generation in Large-Scale Electrification-Planning Problems: A Direct-Search

- Approach,” 2019.
- [21] S. M. Zahraee, M. Khalaji Assadi, and R. Saidur, “Application of Artificial Intelligence Methods for Hybrid Energy System Optimization,” *Renew. Sustain. Energy Rev.*, vol. 66, pp. 617–630, 2016.
- [22] T. Kerdphol, R. N. Tripathi, T. Hanamoto, Khairudin, Y. Qudaih, and Y. Mitani, “ANN based optimized battery energy storage system size and loss analysis for distributed energy storage location in PV-microgrid,” *Proc. 2015 IEEE Innov. Smart Grid Technol. - Asia, ISGT ASIA 2015*, 2016.
- [23] L. Hontoria, J. Aguilera, and P. Zufiria, “A new approach for sizing stand alone photovoltaic systems based in neural networks,” *Sol. Energy*, vol. 78, no. 2, pp. 313–319, 2005.
- [24] A. Dolara, A. Gandelli, F. Grimaccia, S. Leva, and M. Mussetta, “Weather-based machine learning technique for day-ahead wind power forecasting,” *2017 6th Int. Conf. Renew. Energy Res. Appl. ICRERA 2017*, vol. 2017-January, pp. 206–209, 2017.
- [25] R. Al-Hajj, A. Assi, and M. M. Fouad, “A predictive evaluation of global solar radiation using recurrent neural models and weather data,” *2017 6th Int. Conf. Renew. Energy Res. Appl. ICRERA 2017*, vol. 2017-January, pp. 195–199, 2017.
- [26] B. Zhao, X. Zhang, P. Li, K. Wang, M. Xue, and C. Wang, “Optimal sizing, operating strategy and operational experience of a stand-alone microgrid on Dongfushan Island,” *Appl. Energy*, vol. 113, pp. 1656–1666, 2014.
- [27] T. Senjyu, D. Hayashi, A. Yona, N. Urasaki, and T. Funabashi, “Optimal configuration of power generating systems in isolated island with renewable energy,” *Renew. Energy*, vol. 32, no. 11, pp. 1917–1933, 2007.
- [28] L. Cornejo-Bueno, “New Hybrid Neuro-Evolutionary Algorithms for Renewable Energy and Facilities Management Problems,” 2018.
- [29] M. Castañeda, A. Cano, F. Jurado, H. Sánchez, and L. M. Fernández, “Sizing optimization, dynamic modeling and energy management strategies of a stand-alone PV/hydrogen/battery-based hybrid system,” *Int. J. Hydrogen Energy*, vol. 38, no. 10, pp. 3830–3845, 2013.
- [30] F. J. Ardakani, G. Riahy, and M. Abedi, “Design of an optimum hybrid renewable energy system considering reliability indices,” *Proc. - 2010 18th Iran. Conf. Electr. Eng. ICEE 2010*, vol. 1000, pp. 842–847, 2010.
- [31] S. Bayhan, Y. Liu, and S. Demirbas, “A novel energy management algorithm for islanded AC microgrid with limited power sources,” *2017 6th Int. Conf. Renew. Energy Res. Appl. ICRERA 2017*, vol. 2017-January, pp. 64–69, 2017.
- [32] D. Connolly, H. Lund, B. V. Mathiesen, and M. Leahy, “A review of computer tools for analysing the integration of renewable energy into various energy systems,” *Appl. Energy*, vol. 87, no. 4, pp. 1059–1082, 2010.
- [33] W. M. Amutha and V. Rajini, “Cost benefit and technical analysis of rural electrification alternatives in southern India using HOMER,” *Renew. Sustain. Energy Rev.*, vol. 62, pp. 236–246, 2016.
- [34] M. Sharafi and T. Y. ELMekkawy, “Multi-objective optimal design of hybrid renewable energy systems using PSO-simulation based approach,” *Renew. Energy*, vol. 68, pp. 67–79, 2014.
- [35] S. R. Alvarez, A. M. Ruiz, and J. E. Oviedo, “Optimal design of a Diesel-PV-Wind system with batteries and hydro pumped storage in a Colombian community,” in *6th International Conference on Renewable Energy Research and Applications*, 2017, vol. 5.
- [36] K. Kajiwara, N. Matsui, and F. Kurokawa, “A new MPPT control for solar panel under bus voltage fluctuation,” *2017 6th Int. Conf. Renew. Energy Res. Appl. ICRERA 2017*, vol. 2017-Janua, pp. 1047–1050, 2017.
- [37] J. Kennedy and R. Eberhart, “Particle Swarm Optimization,” in *International Conference on Neural Networks*, 1995, vol. 21, no. 2, pp. 221–230.
- [38] Y. Shi and R. C. Eberhart, “Parameter selection in particle swarm optimization,” in *International Conference on Evolutionary Programming*, 1998, vol. 1447, pp. 591–600.
- [39] V. Hlavác, K. G. Jeffery, and J. Wiedermann, *Lecture Notes in Computer Science*, vol. 1716. Springer, 1999.
- [40] A. Kumar, S. Ajith, A. Patrick, and S. Michael, *Intelligent Decision Support Systems for Sustainable Computing*, vol. 705. 2017.